Molecular Structures of Zinc Complexes with Bisbenzimidazole Ligands in Crystals and the Kinetics of Ligand-Exchange Reactions in Their Solutions

Kazuya Ogawa, Kou Nakata, and Kazuhiko Ichikawa*

Division of Material Science, Graduate School of Environmental Earth Science, Hokkaido University, Sapporo 060

(Received March 27, 1997)

Zinc complexes with bisbenzimidazole, $[ZnL(PhCOO)_2]$ **1**, $[ZnLCl_2]$ **2**, and $[ZnL_2]^{2+}$ **3**, have been synthesized, where L = 2,2′-thiodimethylenebis(benzimidazole). Their molecular structures were determined based on X-ray crystal structure and extended X-ray absorption fine structure (EXAFS) analyses. The molecular structure of **1**·1.5DMF shows a distorted tetrahedral geometry around Zn(II) coordinated by each nitrogen atom of two benzimidazolyl groups and each oxygen atom of two benzoate ions. In solutions of **2** or **3**·$(ClO_4)_2$ the same chemical species, $[ZnLCl_2]$ or $[ZnL_2]^{2+}$, exist as in the coordination structure around zinc in each crystal. The combination of ^{13}C NMR data with the most probable molecular structures of zinc complexes in **1**, **2**, and **3**, determined by X-ray crystal structure and EXAFS analyses, allowed us to assign the two different chemical species, $[ZnL(PhCOO)_2]$ and $[ZnL_2]^{2+}$, as the major and minor components, respectively, in a solution of **1**. A kinetic study of the ligand-exchange reaction between $PhCOO^-$ and L was provided us with the lifetimes of the chemical species of $[ZnL(PhCOO)_2]$ and $[ZnL_2]^{2+}$: 66 ms and 10 ms at −10 °C, respectively. The major species produced by a zinc-assisted supramolecular process in solution is the same type of chemical species $[ZnL(PhCOO)_2]$ as in the coordination structure around zinc in the crystal of **1**·1.5DMF. The ESI mass spectra of a solution of **1**, **2**, and **3**·$(ClO_4)_2$ supported the chemical species of $[ZnL(PhCOO)_2]$, $[ZnL_2]^{2+}$, and $[ZnLCl_2]$ in solution.

Studying the non-covalent interactions that occur in synthetic host–guest complexes has been demonstrated to be an effective way to gain insight into the origins of natural binding processes as well as a guide to the design novel supramolecular structures. A target supermolecule may be assembled from a logically chosen precursor molecule or ligands and cations. Here, the zinc ion, which has no ligand field effect associated with a particular coordination geometry, has received great interest from the view of supramolecular architecture. The control over the symmetry and directionality of non-covalent interactions in an artificial ligand can afford very specific control over the coordinated bond with zinc and the coordination position and number around zinc. The biomimetic molecular design of the immediate zinc coordination geometry will enforce the tetrahedral structure around the zinc complex as a model complex[1—9] of an active site of zinc enzyme.[10,11]

In molecular design, zinc should be coordinated by imidazole, carboxylate, a water molecule, and a chloride ion; in the zinc enzyme, the above-mentioned ligands provide some enzymatic function or inhibitor, such as carbonic anhydrase[10] and carboxypeptidaseA.[11] Since the introduction of bulky groups into ligands gives rise to the effect of a steric hindrance and a small coordination number of four, the tetrahedral coordination around zinc can be built from the view of supramolecular architecture.

In this paper, we report on the syntheses of zinc complexes with the ligands of bisbenzimidazole, benzoate ion, and chloride ion, their molecular structures in a crystal, the correlation between the molecular structure in a crystal and the major chemical species in their solutions, and the thermodynamics and kinetics of a ligand-exchange reaction in the first shell around zinc.

Experimental

Syntheses of 2,2′-Thiodimethylenebis(benzimidazole) and 1, 3-Bis(2-benzimidazolyl)propane, L and L′. Ligands were prepared from *o*-phenylenediamine and thiodiglycolic acid for L[12] or glutaric acid for L′.[13] The identity and purity were confirmed by ^1H and ^{13}C NMR spectroscopy and elemental analysis. ^1H NMR (L), δ = (ppm vs. TMS in DMSO-d_6) methylene 4.09 (s, 4H), aromatic 7.16 (m, 4H), 7.53 (m, 4H). ^{13}C NMR (L), δ = (ppm vs. TMS in DMSO-d_6) methylene 28.8, aromatic 115.0, 121.0, 139.0, 154.4. Found: C, 61.39; H, 5.24; N, 17.79%. Calcd for $C_{16}H_{16}N_4OS$, (L·H_2O): C, 61.51; H, 5.16; N, 17.93%. ^1H NMR (L′), δ = (ppm vs. TMS in DMSO-d_6) methylene 2.34 (t, 2H), 2.94 (t, 4H), aromatic 7.08 (m, 4H), 7.44 (m, 4H). ^{13}C NMR (L′), δ = (ppm vs. TMS in DMSO-d_6) methylene 25.9, 28.0, aromatic 114.8, 121.7, 138.7, 151.7. Found: C, 74.00; H, 5.94; N, 20.21%. Calcd for $C_{17}H_{16}N_4$, (L′): C, 73.88; H, 5.83; N, 20.27%.

Syntheses of $[ZnL(PhCOO)_2]$ and $[ZnL'(PhCOO)_2]$, 1 and 1′. (Chart 1). After a MeOH solution of $Zn(PhCOO)_2$ (1.6 mmol) and L (1.6 mmol) was refluxed for 4 h, a white precipitate was filtered. Colorless crystals of **1**·1.5DMF were obtained from a DMF solution. ^1H NMR, δ = (ppm vs. TMS in DMSO-d_6) methylene 4.39 (s), aromatic 7.23 (s), 7.40—7.42 (d), 7.46—7.47 (d), 7.62 (s), 7.97 (t). ^{13}C NMR, δ = (ppm vs. TMS in DMSO-d_6) methylene 25.1, 27.1, aromatic 112.5, 117.5, 121.7, 123.3, 128.0, 129.3,

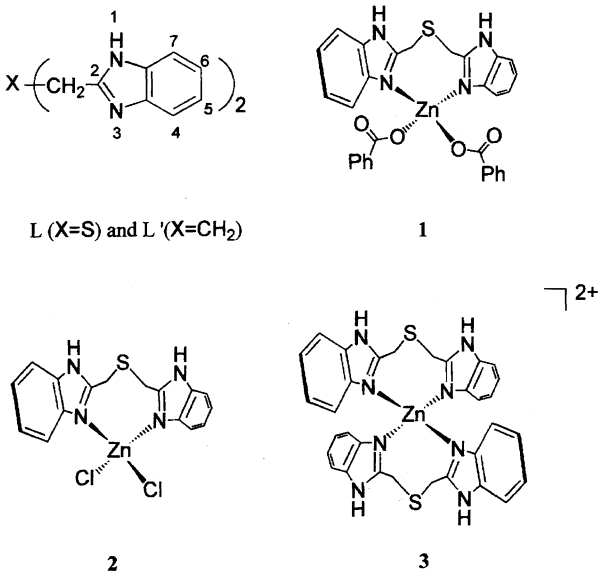

Chart 1.

131.2, 133.0, 134.6, 139.9, 141.8, 152.5, carboxylate 170.0. Found: C, 57.99; H, 4.49; N, 10.76%. Calcd for $C_{34.5}H_{34.5}N_{5.5}O_{5.5}SZn$, ([ZnL(PhCOO)$_2$]·1.5DMF): C, 58.22; H, 4.88; N, 10.82%. **1′** was synthesized by the method similar to **1**. ^{1}H NMR, δ = (ppm vs. TMS in DMSO-d_6) methylene 2.12 (s), 3.20 (s), aromatic 7.13—7.98. ^{13}C NMR, δ = (ppm vs. TMS in DMSO-d_6) methylene 24.5, 27.6, aromatic 111.6, 117.6, 120.9, 123.0, 127.6, 129.3, 130.7, 132.5, 134.7, 139.7, 142.0, 152.2, carboxylate 170.4. Found: C, 61.75; H, 4.84; N, 9.17%. Calcd for $C_{31}H_{26}N_4O_4Zn$, ([ZnL′(PhCOO)$_2$] 1.5CH$_3$OH): C, 61.76; H, 5.10; N, 8.86%.

Synthesis of [ZnLCl$_2$], 2. A MeOH solution of $ZnCl_2$ (1.6 mmol) was added into a hot MeOH solution of L (1.6 mmol). Immediately, a white precipitate was formed. ^{1}H NMR, δ = (ppm vs. TMS in DMSO-d_6) methylene 4.06 (s, 4H), aromatic 7.38 (s, 4H), 7.70 (s, 2H), 8.29 (s, 2H). ^{13}C NMR, δ = (ppm vs. TMS in DMSO-d_6) methylene 25.5, aromatic 113.0, 119.0, 124.0, 133.0, 139.0, 152.0. Found: C, 44.80; H, 3.46; N, 13.01%. Calcd for $C_{16}H_{14}Cl_2N_4SZn$, ([ZnLCl$_2$]): C, 44.62; H, 3.27; N, 13.00%.

Synthesis of [ZnL$_2$](ClO$_4$)$_2$, 3·(ClO$_4$)$_2$. A hot MeOH solution of Zn(ClO$_4$)$_2$·6H$_2$O (1.6 mmol) and L (1.6 mmol) was stirred for 30 min. After several days, colorless crystals of **3**·(ClO$_4$)$_2$ grew from the reaction solution. ^{1}H NMR, δ = (ppm vs. TMS in DMSO-d_6) methylene 4.17 (s, 4H), aromatic 7.24—7.27 (m, 4H), 7.52—7.55 (m, 4H). ^{13}C NMR, δ = (ppm vs. TMS in DMSO-d_6) methylene 27.3, aromatic 115.1, 123.8, 137.1, 152.7. Found: C, 42.73; H, 3.83; N, 12.18%. Calcd for $C_{33}H_{36}Cl_2N_8O_{11}S_2Zn$, ([ZnL$_2$]-(ClO$_4$)$_2$·2H$_2$O·CH$_3$OH): C, 43.03; H, 3.94; N, 12.16%.

Single Crystal X-Ray Diffraction Analysis. A crystal of **1**·1.5DMF for an X-ray diffraction measurement was obtained by slow evaporation of a DMF solution of **1**. The measurement was made on a Rigaku AFC7R diffractometer with Cu $K\alpha$ radiation at 23 °C. The intensities of three standard reflection were measured every 100 reflections. Over the course of data collection, the standards decreased by 5.5%. A linear correction was applied to the data. The crystal data and experimental details are summarized in Table 1.

The structure was solved by direct methods and expanded using Fourier techniques with DIRDIF92.[14] The non-hydrogen atoms were refined anisotropically. Hydrogen atoms were included, but not refined. The fractional atomic coordinates and equivalent isotropic displacement of non-hydrogen atoms are given in Table 2.

Table 1. Crystal Data for **1**·1.5DMF

Formula	$ZnC_{34.5}H_{34.5}N_{5.5}O_{5.5}S$
FW	711.63
Crystal size	0.35×0.30×0.20 mm
Crystal system	Triclinic
Lattice parameters	a = 11.481(2)Å
	b = 15.516(6)Å
	c = 11.021(2)Å
	α = 94.56(3)°
	β = 114.74(1)°
	γ = 94.81(2)°
	V = 1762.5(8)Å^3
Space group	$P\bar{1}$
Z	2
d_{calcd}	1.341 g cm^{-3}
Diffractometer	Rigaku AFC7R
Radiation	Cu $K\alpha$ (λ = 1.54178 Å)
Temperature	23±1 °C
Scan type	ω–2θ
2θ_{max}	120.2°
No. of reflcns measd	5484
No. of obsvatns ($I > 3\sigma(I)$)	4614
No. of variables	362
R, R_w	0.040,[a] 0.068[b]

a) $R = \Sigma||F_o| - |F_c||/\Sigma|F_o|$. b) $R_w = (\Sigma w(|F_o| - |F_c|)^2/\Sigma wF_o^2)^{1/2}$, $w = [\sigma^2(F_o) + 0.001444F_o^2]$.

Extended X-Ray Absorption Fine Structure (EXAFS) Analysis. The X-ray absorption spectra at the Zn K-edge were recorded on a Rigaku R-2000 system with radiation generated by a rotating target of Ag. The transmission mode was employed using an ionization chamber and a scintillation counter for I_0 and I detection, respectively. The EXAFS function ($\chi(E)$) from the corrected absorption spectra was converted into $\chi(\boldsymbol{k})$ according to

$$\boldsymbol{k} = [8\pi^2 m(E - E_0)/h^2]^{1/2}, \quad (1)$$

where m is the mass of an electron and E_0 is the energy of the Zn K-edge (ca. 9660 eV). The $\boldsymbol{k}^3$-weighted EXAFS data of **1**,**2**, and **3**·(ClO$_4$)$_2$ at the zinc K-edge are presented in Fig. 1. A Fourier transformation of $\boldsymbol{k}^3$-weighted $\chi(\boldsymbol{k})$ was made over the region from 3.5 to 12.0 Å^{-1}. The first-shell EXAFS data obtained from the back-transformation were simulated for each sample according to

$$\chi(\boldsymbol{k}) = \Sigma n_j f(\boldsymbol{k}) \exp(-2\sigma_j^2 \boldsymbol{k}^2) \cdot \sin(2\boldsymbol{k}r_j + \phi(\boldsymbol{k}))/\boldsymbol{k}r_j^2, \quad (2)$$

where n_j, σ_j, and r_j are the number of scatters, the Debye–Waller factor containing static and thermal contributions, and the zinc-scatter distance for each nucleus (j), respectively. The back-scattering amplitude function ($f(\boldsymbol{k})$) and the phase function ($\phi(\boldsymbol{k})$), calculated by an ab initio method,[15] were used.

^{13}C NMR Measurements. The ^{13}C NMR spectra were measured by using a JEOL EX-400 spectrometer (100.5 MHz). The solvent was DMSO-d_6/CDCl$_3$ (1 : 1, v/v).[16] The chemical shifts are indicated vs. TMS. The sample concentration was adjusted to 0.1 and 0.2 M.

Electrospray Ionization (ESI) Mass Spectra Measurements. The ESI mass spectra were measured at ca. 10^{-5} M in DMSO/CHCl$_3$ (1 : 1, v/v) (1 M = 1 mol dm^{-3}). The nature of these product ions, which gave rise to the observed bands in ESI mass spectrum, may depend upon the composition and feed rate of

Table 2. Fractional Atomic Coordinates and Equivalent Isotropic Thermal Parameters for **1**·1.5DMF

Atom	x	y	z	B_{eq}
Zn(1)	0.53689(3)	0.76756(2)	0.18969(3)	3.390(9)
S(1)	0.62182(9)	0.79424(7)	−0.14845(8)	5.87(2)
O(1)	0.37262(2)	0.7780(1)	0.2025(2)	4.32(2)
O(2)	0.3195(3)	0.8622(3)	0.0454(4)	11.4(1)
O(3)	0.6372(2)	0.7405(1)	0.3725(2)	4.52(4)
O(4)	0.7899(2)	0.7217(1)	0.3045(2)	5.07(5)
O(5)	0.5854(4)	0.5213(3)	−0.3074(4)	10.3(1)
O(6)	0.3993(6)	1.0130(4)	0.2455(6)	8.0(2)
N(1)	0.4874(2)	0.6717(1)	0.0347(2)	4.10(5)
N(2)	0.4909(3)	0.5866(2)	−0.1350(2)	5.36(6)
N(3)	0.6232(2)	0.8784(1)	0.1640(2)	3.82(5)
N(4)	0.6733(3)	0.9857(2)	0.0671(3)	5.40(7)
N(5)	0.6537(4)	0.4245(2)	−0.4148(3)	7.38(9)
N(6)	0.498(1)	1.019(1)	0.468(2)	7.9(5)
C(1)	0.5488(3)	0.657(2)	−0.0420(3)	4.52(6)
C(2)	0.3820(3)	0.6062(2)	−0.0108(3)	4.48(6)
C(3)	0.2877(3)	0.5887(2)	0.0332(4)	5.48(7)
C(4)	0.1957(3)	0.5158(2)	−0.0334(5)	6.92(9)
C(5)	0.2017(4)	0.4639(2)	−0.1406(5)	7.6(1)
C(6)	0.2941(4)	0.4810(2)	−0.1846(4)	6.77(9)
C(7)	0.3859(3)	0.5531(2)	−0.1178(3)	5.36(7)
C(8)	0.6627(3)	0.7120(2)	−0.0332(3)	5.01(7)
C(9)	0.5282(3)	0.8583(2)	−0.0855(3)	4.99(7)
C(10)	0.6069(3)	0.9067(2)	0.0476(3)	4.39(7)
C(11)	0.7056(3)	0.9433(2)	0.2647(3)	4.40(6)
C(12)	0.7546(3)	0.9492(2)	0.4047(4)	5.69(8)
C(13)	0.8342(4)	1.0232(3)	0.4778(5)	7.6(1)
C(14)	0.8676(5)	1.0901(3)	0.4146(7)	8.6(1)
C(15)	0.8189(4)	1.0860(2)	0.2778(6)	7.7(1)
C(16)	0.7375(3)	1.0115(2)	0.2027(4)	5.5(8)
C(17)	0.2973(3)	0.8244(2)	0.1277(3)	5.09(7)
C(18)	0.1757(3)	0.8332(2)	0.1438(3)	4.84(7)
C(19)	0.1336(3)	0.7753(2)	0.2083(3)	5.21(7)
C(20)	0.0222(3)	0.7848(3)	0.2259(4)	6.33(9)
C(21)	−0.0447(3)	0.8517(3)	0.1826(5)	6.9(1)
C(22)	−0.0034(5)	0.9097(4)	0.1200(6)	10.2(2)
C(23)	0.1060(4)	0.9001(4)	0.0976(6)	9.9(2)
C(24)	0.7520(3)	0.7254(2)	0.3923(3)	3.83(6)
C(25)	0.8415(3)	0.7145(2)	0.5343(3)	4.17(6)
C(26)	0.8170(3)	0.7438(3)	0.6416(3)	5.96(8)
C(27)	0.9019(4)	0.7364(3)	0.7727(4)	7.4(1)
C(28)	1.0118(4)	0.6989(3)	0.7959(4)	7.4(1)
C(29)	1.0375(4)	0.6680(3)	0.6914(5)	7.4(1)
C(30)	0.9522(3)	0.6768(2)	0.5587(4)	5.65(8)
C(31)	0.5695(6)	0.4455(4)	−0.3662(5)	9.3(2)
C(32)	0.6139(9)	0.3370(5)	−0.4908(7)	14.2(3)
C(33)	0.758(1)	0.4724(8)	−0.407(1)	19.7(4)
C(34)	0.435(1)	0.9802(7)	0.353(1)	7.0(2)
C(35)	0.548(1)	1.1108(7)	0.4919(9)	8.1(3)
C(36)	0.536(4)	0.969(3)	0.573(4)	15(1)

$B_{eq}=8\pi^2(U_{11}(aa^*)^2+U_{22}(bb^*)^2+U_{33}(cc^*)^2+2U_{12}aa^*bb^*\cos\gamma+2U_{13}aa^*cc^*\cos\beta+2U_{23}bb^*cc^*\cos\alpha)/3$.

the original solution, the temperature and composition of the bath gas, and the voltage applied to the capillary.

Results and Discussion

Molecular Structure of 1, 2, and 3. An ORTEP drawing of **1**·1.5DMF and selected bond lengths and bond angles for

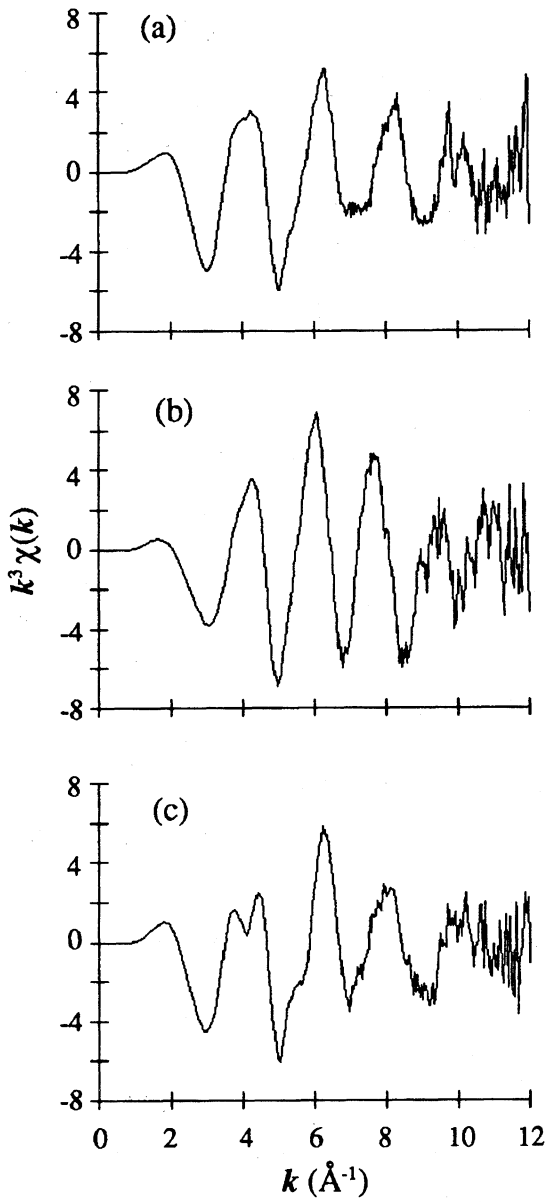

Fig. 1. k^3-Weighted fine structure at the Zn K-edge of (a) **1**, (b) **2**, and (c) **3**·$(ClO_4)_2$.

the molecular structure of **1** are given in Fig. 2 and Table 3, respectively. The zinc ion in the crystal state of **1**·1.5DMF is coordinated by each nitrogen atom of two benzimidazoles and each oxygen atom of two benzoate ions. The coordination geometry around a zinc ion is tetrahedral, as shown in general zinc complexes. The average bond lengths from the zinc ion to nitrogen and oxygen atoms are 2.018 and 1.963 Å, respectively: Other distances of Zn–O(2) and Zn–O(4) are 2.929 and 2.821 Å, respectively, which are longer than the bond lengths between the zinc ion and oxygen atoms O(1) and O(3). Consequently, the coordination of each carboxylate of two benzoate ions is characteristic of monodentate. The distinction between monodentate and bidentate coordination of carboxylate to Zn(II) can also be estimated by separating the vibration energy ($\Delta\nu$=213 cm^{-1}) between ν_a(COO) at 1596

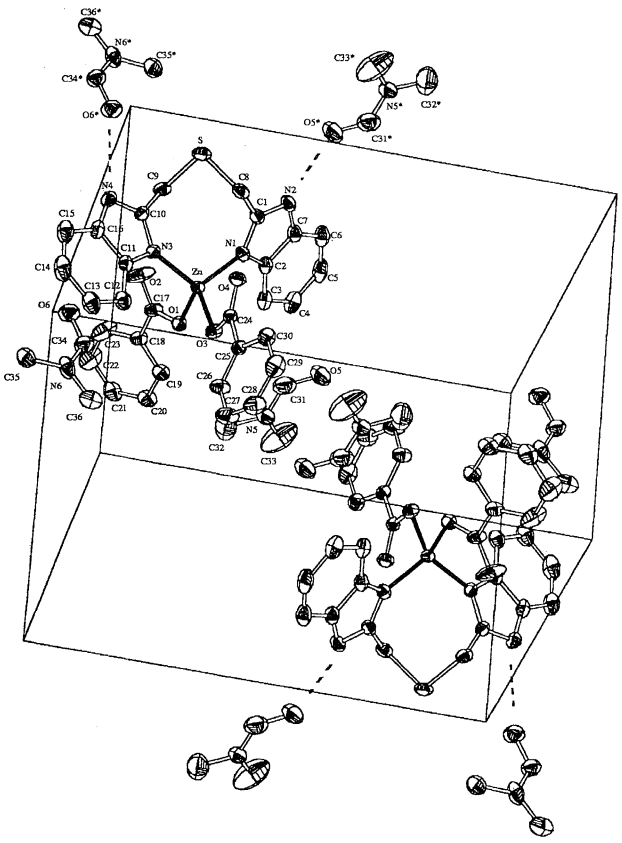

Fig. 2. ORTEP drawing atom-numbering system of **1**·1.5DMF. The numbers with an asterisk indicate the DMF molecules drawn by symmetric operation. Ellipsoids are depicted at the 20% probability level.

Table 3. Selected Bond Distances (Å) and Bond Angles (deg) for **1**

Zn—O(1)	1.968(2)	Zn—O(3)	1.958(2)
Zn—N(1)	2.024(2)	Zn—N(3)	2.011(2)
Zn···O(2)	2.929(4)	Zn···O(4)	2.821(2)
O(1)—Zn—O(3)	98.01(8)	O(1)—Zn—N(1)	103.24(8)
O(1)—Zn—N(3)	114.96(8)	O(3)—Zn—N(1)	118.06(9)
O(3)—Zn—N(3)	108.77(9)	N(1)—Zn—N(3)	113.00(9)

cm^{-1} and ν_s(COO) at 1383 cm^{-1}. Monodentate for the carboxylate ligand to Zn(II) possesses a value of $\Delta\nu$ greater than 200 cm^{-1}.[17] The zinc exists in the plane made by carboxylate group; the distances from the planes of O(1)–C(17)–O(2) and O(3)–C(24)–O(4) to the zinc ion and the dihedral angle between their planes are 0.042, 0.175 Å, and 30.99°, respectively. The two protons of the benzimidazole N–H groups form hydrogen bonds with oxygen atoms of DMF: N(2)–H···O(5*)=2.723 Å and N(4)–H···O(6*)=3.190 Å, as shown in Fig. 2.

The coordination structures around the zinc ion of **1**, **2**, and **3** were determined by EXAFS analysis, as shown in Table 4. The coordination numbers for N, O, and Cl were fixed at the initial step of curve-fitting analyses for the EXAFS data of **1**, **2**, and **3**. For the EXAFS analysis of **1**, the preliminary distances from zinc to the two oxygen atoms and the two nitrogen atoms were obtained, where the coordination numbers for oxygen and nitrogen were given from the X-ray crystallographic structure of **1** (Fig. 2). The coordination structure around zinc in the **1**·1.5DMF crystal corresponded to the structural formula [ZnL(PhCOO)$_2$], determined by elemental analysis, ^{1}H/^{13}C NMR, and IR spectra, as shown in the synthesis of **1**. The zinc ion in **2**, the structural formula [ZnLCl$_2$] of which was determined from the elemental analysis and ^{1}H/^{13}C NMR, is coordinated by two nitrogen atoms and two chloride ions, as shown in Table 4. The distance between the zinc ion and the nitrogen atoms is close to that of **1**: the Zn–Cl distances in **2** correspond to the reference data of four coordinate zinc complexes (2.25—2.29 Å[18]). Thus, the geometry around the zinc ion in **2** is characteristic of the tetrahedral arrangement. The elemental analysis of **3**·(ClO$_4$)$_2$ predicted that the constitution of **3** is 1 : 2 (=Zn : L). Since the ^{1}H/^{13}C NMR spectra were independent of counter ions, as mentioned below, the zinc ion is coordinated by four nitrogen atoms and never by ClO_4^-. A least-squares fitting of the EXAFS data of **3** converged with a Zn–N distance of ca. 2.0 Å at a given coordination number of four nitrogen atoms. The final coordination-numbers and distances were obtained by further optimization of curve-fitting analyses for the first shell EXAFS data, as shown in Table 4. Since **2** consists of two monatomic ions of Cl^-, the value, 0.018, of R defined in Table 4, was smaller than those of **1** and **3**. The good agreement between the structural parameters of single-crystal X-ray and EXAFS data for **1** demonstrates the

Table 4. Results of Curve Fitting Analysis of the First Shell EXAFS Data for **1**, **2**, and **3**·(ClO$_4$)$_2$

Sample	Window width/Å	Scatterer	n	r/Å	σ/Å	R[1]
1	0.8—2.1	N	2.1	2.0_5 (2.018)[2]	0.05	0.091
		O	2.0	1.9_5 (1.963)[2]	0.07	
2	1.1—2.4	N	2.1	2.0_5	0.04	0.018
		Cl	2.1	2.3_0	0.06	
3·(ClO$_4$)$_2$	1.0—2.5	N	3.7	2.0_5	0.08	0.177

1) $R=\Sigma[k_i^3\chi^{obs}(k_i)-k_i^3\chi^{calc}(k_i)]^2/\Sigma[k_i^3\chi^{obs}(k_i)]^2$. 2) Averages of bond length in the crystal structure of **1**.

reasonable and correct analyses for EXAFS data of **2** and **3**.

The O(1)–Zn–O(3) and N(1)–Zn–N(3) bond angles of 98.01 and 113.00° show a distortion of **1** from regular tetrahedral with a steric hindrance among four benzene rings of benzimidazoles and benzoate ions; the model complex $[Zn(RCOO)_2(Im)_2]$ ($R=CH_3$, C_2H_5)[5] of carboxypeptidase A doesn't show any significant distortion (i.e. their angles are 105.8 and 110.2°, respectively) because of a small steric hindrance. These benzene rings also provide a hydrophobic environment around a zinc ion. The minimum-energy structure around the zinc ion in **2** or **3** was obtained by a MM2 calculation of molecular mechanics[19] with optimized and reliable data of the nearest-neighbor distances and the coordination numbers (see Table 4), as shown in Fig. 3.

The X-ray crystallographic data of **1** showed that the distance between the zinc ion and the sulfur atom in an eight-membered chelate ring is 4.270 Å. Also, for EXAFS analyses of **1**, **2**, and **3**·$(ClO_4)_2$, there is no scattering contribution from the sulfur atom around Zn(II) within 2.5 Å. On the other hand, the zinc complex, which was coordinated by thioether ligands without nitrogen and oxygen atoms, showed a distance of 2.6 Å between zinc and sulfur atom.[18] It is well known that (1) Zn^{2+} can't be stabilized by the effect of the ligand field because of its d^{10} electronic structure and (2) Zn^{2+} is classified as in the intermediate Lewis acid by the rule of HSAB. Thus, Zn^{2+} prefers to be coordinated by nitrogen atoms and oxygen atoms rather than a soft sulfur atom; the dependence of the ^{13}C NMR spectra of a solution of **1'**, where $X=CH_2$ instead of a sulfur atom, showed the same shifts and intensities compared with that of **1** (X=S).

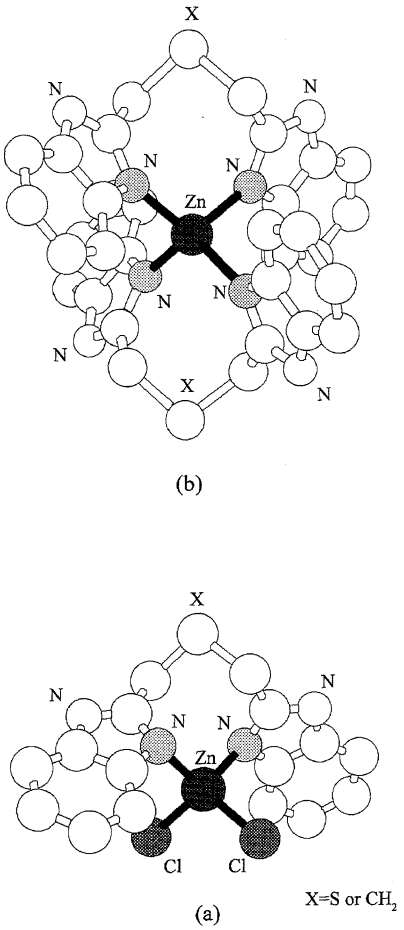

Fig. 3. Molecular structures optimized by MM2 calculation for (a) 1 : 1 species of **2** and (b) 1 : 2 species of **3**.

Chemical Species in a Solution of 1. The ^{13}C NMR spectra of **1** in solution show two chemical species of the zinc complexes; **2** and **3**·$(ClO_4)_2$ show only one species in solution, as shown in Fig. 4. Zinc complexes accompanied with L exist as 1 : 1 (=Zn : L) or 1 : 2 species in the solid state. However, the zinc complex in the solid state is not always maintained in solution, because a chemical-exchange

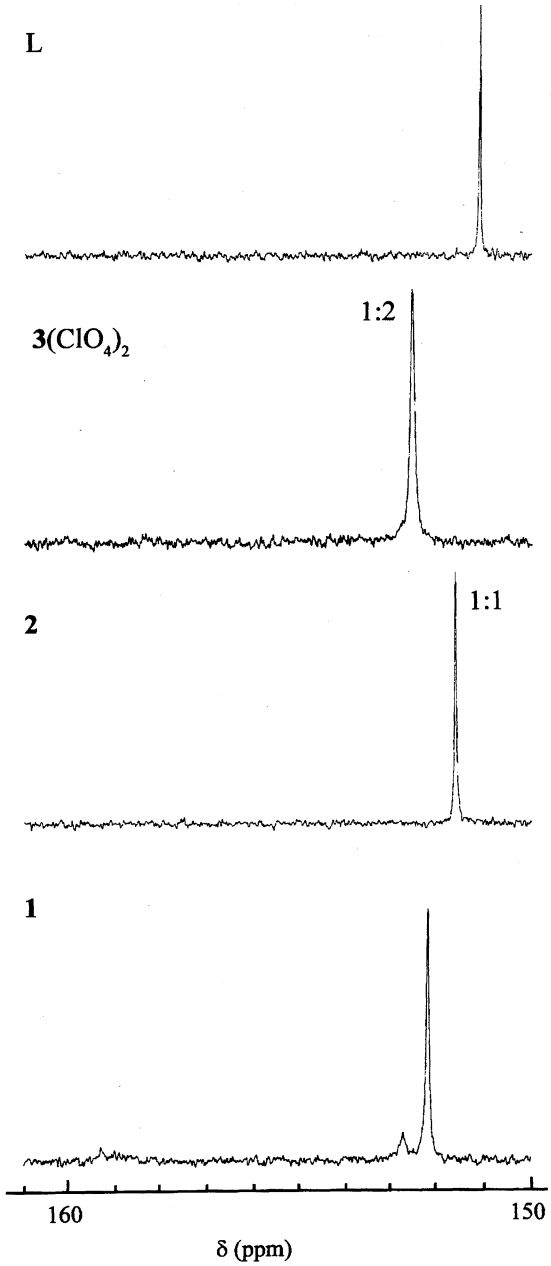

Fig. 4. ^{13}C NMR spectra of **1**, **2**, **3**·$(ClO_4)_2$, and free L for second position of benzimidazole rings in DMSO-d_6/$CDCl_3$ at −10 °C and 0.2 M.

reaction often occurs between L and $PhCOO^-$ based on the ^{13}C NMR spectra of **1** in DMSO-d_6/$CDCl_3$ at -10 °C (see Fig. 4). The fact that the ^{13}C of the second position of benzimidazole rings separates into two signals, 152.3 and 152.8, demonstrates the two chemical species in the solution of **1**. Since the two signals are shifted downfield by 1.2 and 1.7 ppm from free L ($\delta=151.1$), respectively, the two chemical species are both zinc-bound L. The ^{13}C NMR spectra for the second position of the benzimidazole ring of **2** or **3**·$(ClO_4)_2$, which were measured in order to identify these chemical species, showed a single peak at $\delta=151.6$ or 152.7, respectively, indicating just one chemical species for the zinc complex in a solution of **2** or **3**·$(ClO_4)_2$. Since the most stable conformations around Zn(II) were identified as mentioned above, each zinc complex in a solution of **2** or **3**·$(ClO_4)_2$ can be assigned to 1 : 1 (i.e. Zn : L) or 1 : 2 species, which corresponds to (a) or (b) in Fig. 3. The much smaller ^{13}C NMR peak at $\delta=152.8$ for a solution of **1** (see Fig. 4) is equivalent to 1 : 2 species (i.e., (a) in Fig. 3), because of the good agreement with the chemical shift, $\delta=152.7$, of the 1 : 2 species for a solution of **3**·$(ClO_4)_2$ within the experimental error. The ^{13}C NMR shifts for the solutions of **3**·$(NO_3)_2$, **3**·$(CF_3SO_3)_2$, and **3**·$(ClO_4)_2$ have been shown to be almost the same as each other, and to be no concentration dependence between 0.1 M **3**·X_2 and 0.2 M. Here, the bulky counter-ions, such as NO_3^-, $CF_3SO_3^-$, and ClO_4^-, do not show any effect on the complexation of zinc with the two Ls. The big ^{13}C NMR shift at $\delta=152.3$ means the most probable species in solution and results from the zinc complex 1 : 1 species, which corresponds to the most probable coordination of L and two benzoate ions around Zn(II), as shown in crystalline structure of Fig. 2. The reason why the small, but significant, difference in the ^{13}C NMR shifts (0.7 ppm) has been observed between the 1 : 1 species formed by **1** and **2** lies with the difference of the second ligands, $PhCOO^-$ and Cl^-.

In addition, the ESI mass spectra provided final unequivocal evidence for the assignment of chemical species of **1**, **2**, and **3**·$(ClO_4)_2$ in the solution or gas phase, as shown in Fig. 5. They displayed common-type bands at m/z=295, 357, and 393, corresponding to the cationic species L, [ZnL]Cl, and $[ZnL_2]Cl$, respectively. Since the bands have been observed at m/z=757 for **1**, 825 for **2**, and 851/751 for **3**·$(ClO_4)_2$, they originated from the most-probable molecular structures in crystal or the major chemical species in solution. Here, a mass-spectrometric analysis showed that these species became bigger in aggregation with solvent molecules (i.e., dimethyl sulfoxide) or counter ions (i.e., ClO_4^- or Cl^-/Cl).

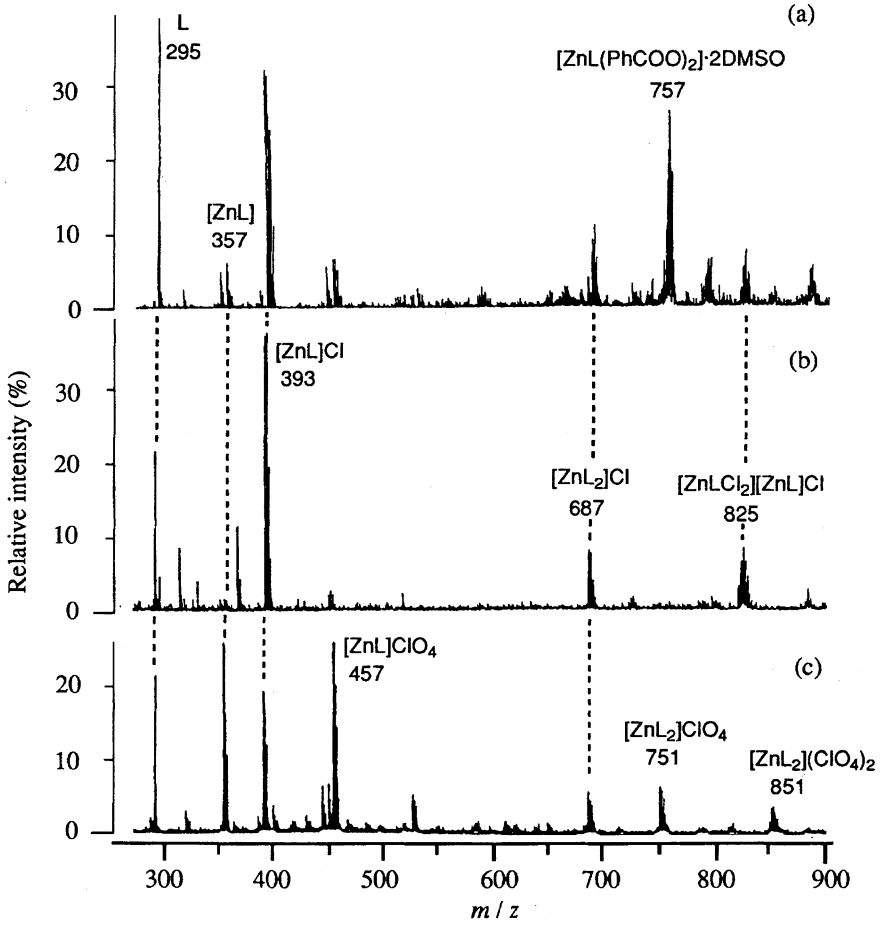

Fig. 5. Electrospray ionization mass spectra of (a) **1**, (b) **2**, and (c) **3**·$(ClO_4)_2$ in DMSO/$CHCl_3$. The chlorine atom in some fragments was supplied by the decomposition of $CHCl_3$.

The spectra of ^{13}C NMR of a solution of **1** were independent of the solvents, such as dimethyl sulfoxide and *N,N*-dimethylformamide. The coordinate bond of the sulfoxide or carboxyamide group with Zn(II) is very weak compared with the carboxylate ion as well as the chloride ion. In conclusion, the ^{13}C NMR data with two peaks, which were reliably observed and assigned for the solution of **1** (see Fig. 4), excluded the chemical species partially coordinated by DMSO.

Kinetics of Exchange Reaction of Ligands. The temperature dependence of the ^{13}C NMR spectra for the second position of benzimidazole rings of **1** in solution (see the left side of Fig. 6) shows that there is the ligand-exchange reaction between the $[ZnL(PhCOO)_2]$ and $[ZnL_2]^{2+}$ species. The chemical reaction in solution can be written as

$$2[ZnL(PhCOO)_2] \rightleftharpoons [ZnL_2]^{2+} + Zn^{2+} + 4PhCOO^- . \quad (3)$$

In the case of ^{13}C NMR (Fig. 6), the ligand-exchange reaction between the benzoate ion and L, Eq. 3, can be simplified as[20,21]

$$^{13}C\{in\,[ZnL(PhCOO)_2]\} \rightleftharpoons {}^{13}C\{in\,[ZnL_2]^{2+}\}. \quad (4)$$

Since local equilibrium between the main $[ZnL(PhCOO)_2]$ and $[ZnL_2]^{2+}$ species has been established in the solution of **1**, the relation between their lifetimes (τ_{ZnL} and τ_{ZnL_2}) and the fractional populations of ^{13}C nuclei at the second position of benzimidazole rings (f_{ZnL} and f_{ZnL_2}) is expressed as

$$\tau_{ZnL} f_{ZnL_2} = \tau_{ZnL_2} f_{ZnL}. \quad (5)$$

The simulated ^{13}C NMR spectra are shown on the right side of Fig. 6.[22]

When **1** was dissolved into solution at $-10\,^{\circ}C$, two signals of ^{13}C NMR were observed separately, as mentioned above. This fact indicates that the lifetimes of each chemical species

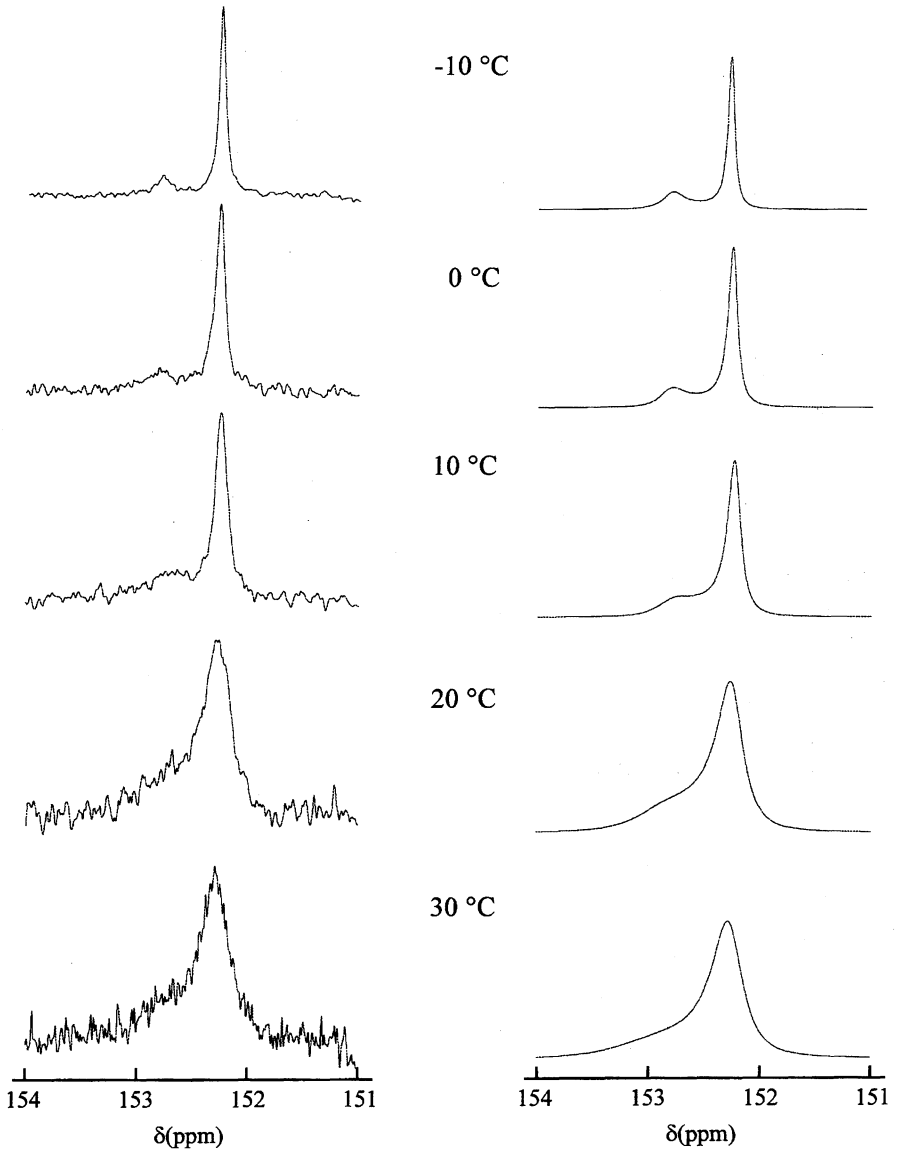

Fig. 6. The observed (left side) and simulated (right side) spectra of ^{13}C NMR for ligand exchange between $[ZnL(PhCOO)_2]$ and $[ZnL_2]^{2+}$ in DMSO-d_6/$CDCl_3$ solution of **1**.

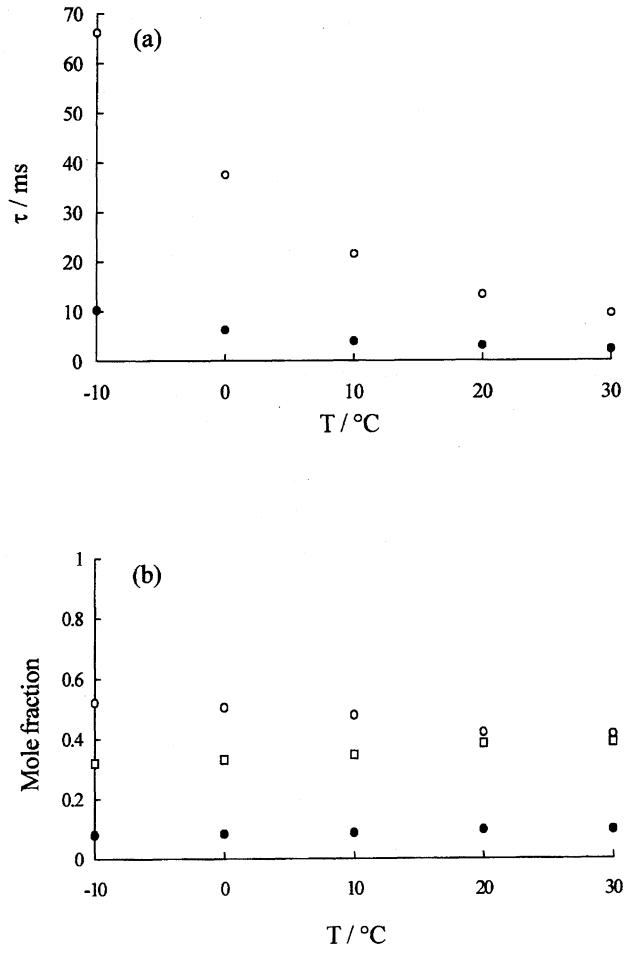

Fig. 7. a) Lifetime (τ) and (b) mole fraction of each chemical species, $[ZnL(PhCOO)_2]$ (○), $[ZnL_2]^{2+}$ and Zn^{2+} (●), and $PhCOO^-$ (□), appeared in Eq. 3, in the solution of **1**.

in solution are long, as shown in Fig. 7(a) (τ_{ZnL}=66 ms, τ_{ZnL_2}=10 ms at −10 °C; τ_{ZnL}=10 ms, τ_{ZnL_2}=2 ms at 30 °C). The difference between the fractional populations of each species becomes smaller as the temperature increases (see Fig. 7(b)); the $[ZnL(PhCOO)_2]$ species still exists four-times more than the $[ZnL_2]^{2+}$ species in the solution, even at 30 °C. The IR spectra of the solution of **1** showed that the coordination of each carboxylate of two benzoate ions was characteristic of monodentate (ν_a(COO)=1629 cm^{-1}, ν_s(COO)=1370 cm^{-1}, and $\Delta\nu$=259 cm^{-1}).

The equilibrium constants of Eq. 3 were obtained from the law of conservation of mass, electrical neutrality condition, and fractional populations of $[ZnL(PhCOO)_2]$ and $[ZnL_2]^{2+}$ species for Eq. 4, i.e. $f_{ZnL}/[f_{ZnL}+f_{ZnL_2}/2]$ and $1-f_{ZnL}/[f_{ZnL}+f_{ZnL_2}/2]$ for each temperature; $K=1.8\times10^{-6}$ (−10 °C), 2.6×10^{-6} (0 °C), 4.1×10^{-6} (10 °C), 1.3×10^{-5} (20 °C), 1.5×10^{-5} M^4 (30 °C), $\Delta H°=38\pm5$ kJ mol^{-1}, $\Delta S°=35\pm20$ J K^{-1} mol^{-1}, and $\Delta G°=29\pm5$ kJ mol^{-1} (−10 °C). The forward reaction in Eq. 3 is endothermic with a large change of entropy.

The ^{13}C NMR spectra for carboxylate of benzoate of **1** at −10 °C spilt into two signals (δ=170.6 and 171.2), whose peak intensities are roughly equal to each other and almost

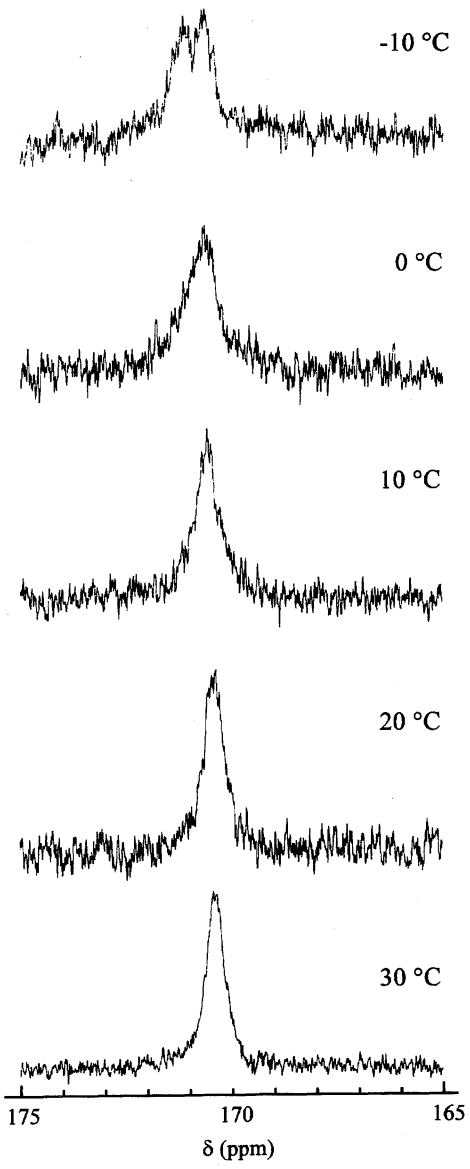

Fig. 8. The temperature dependence of ^{13}C NMR spectra of carboxylate in the solution of **1**.

coalesce at 10 °C, as shown in Fig. 8. Since the mole fraction of free benzoate is very small compared with zinc-bound benzoate in a solution of **1**, the split peaks do not correspond to free and zinc-bound benzoates, respectively. The two different major-sites for zinc-bound benzoates may originate from different coordination geometries of two carboxylate ions around zinc. The coalescence between the split peaks has come from the effects of a ligand-exchange reaction as well as the internal motion of benzoate around zinc.

In conclusion, ligands have been designed and synthesized to keep the tetrahedral coordination around zinc in a zinc-assisted assembling process. The most probable species in a solution of **1** has resulted from the zinc complex coordinated by L and two benzoate ions, as like the most probable coordination-structure around zinc in crystalline **1**.

The ESI mass spectra were measured at GC-MS and NMR

Laboratory, Faculty of Agriculture, Hokkaido University.

References

1) R. S. Brown, N. J. Curtis, and J. Huguet, *J. Am. Chem. Soc.*, **103**, 6953 (1981).
2) W. D. Horrocks, Jr., J. N. Ishley, and R. R. Whittle, *Inorg. Chem.*, **21**, 3265 (1982).
3) A. Looney and G. Parkin, *Inorg. Chem.*, **33**, 1234 (1994).
4) S. Kawabata, K. Nakata, and K. Ichikawa, *Acta Crystallogr., Sect. C*, **C51**, 1554 (1995).
5) N. Kitajima, S. Hikichi, M. Tanaka, and Y. Moro-oka, *J. Am. Chem. Soc.*, **115**, 5496 (1993).
6) A. Looney, R. Han, K. McNeill, and G. Parkin, *J. Am. Chem. Soc.*, **115**, 4690 (1993).
7) T. Koike, M. Inoue, E. Kimura, and M. Shiro, *J. Am. Chem. Soc.*, **118**, 3091 (1996).
8) C. Benelli, I. Bertini, M. D. Vaira, and F. Maini, *Inorg. Chem.*, **23**, 1422 (1984).
9) C. Bazzicalupi, A. Bencini, F. Corana, V. Fusi, C. Giorg, P. Paoli, P. Paoletti, B. Valtancoli, and C. Zanehini, *Inorg. Chem.*, **35**, 5540 (1996).
10) S. K. Nair and D. W. Chiristianson, *J. Am. Chem. Soc.*, **113**, 9455 (1991).
11) D. C. Rees, M. Lewis, and W. N. Lipscomb, *J. Mol. Biol.*, **168**, 367 (1983).
12) H. P. Berends and D. W. Stephan, *Inorg. Chim. Acta*, **93**, 173 (1984).
13) G. A. van Albada, M. T. Lakin, N. Veldman, A. L. Spek, and J. Reedijk, *Inorg. Chem.*, **34**, 4910 (1995).
14) P. T. Beurskens, G. Admiraal, G. Beurskens, W. P. Bosman, R. de Gelder, R. Israel, and J. M. M. Smits, "The DIRDIF-94 Program System, Technical Report of the Crystallography Laboratory," University of Nijmegen.
15) A. G. McKale, B. W. Veal, A. P. Paulikas, S. K. Chan, and G. S. Knapp, *J. Am. Chem. Soc.*, **110**, 3763 (1988).
16) J. C. Lockhart, W. Clegg, M. N. S. Hill, and D. J. Rushton, *J. Chem. Soc., Dalton Trans.*, **1990**, 3541.
17) a) K. Nakamoto, "Infrared and Raman Spectra of Inorganic and Coordination compounds," John Wiley and Sons, New York (1986); b) S. D. Robinson and M. F. Uttley, *J. Chem. Soc., Dalton Trans.*, **1973**, 1913.
18) A. G. Orpen and L. Brammer, *J. Chem. Soc., Dalton Trans.*, Supplement (1989).
19) A molecular mechanics (MM2) package provided by CAChe Scientific, Inc., Version 3.71.
20) K. Ichikawa, T. Jin, and T. Matsumoto, *J. Chem. Soc., Faraday Trans.*, **85**, 175 (1989).
21) T. Jin and K. Ichikawa, *J. Phys. Chem.*, **95**, 2602 (1991).
22) e.g.: K. Ichikawa and T. Matsumoto, *J. Magn. Reson.*, **63**, 445 (1985).
23) K. Nakata, M. K. Uddin, K. Ogawa, and K. Ichikawa, *Chem. Lett.*, **1997**, 991.